Pergamon

Bioorganic & Medicinal Chemistry 10 (2002) 1367–1372

BIOORGANIC & MEDICINAL CHEMISTRY

3-D-QSAR Analysis of *N*-(3-Acyloxy-2-benzylpropyl)-*N*′-dihydroxytetrahydrobenzazepine and Tetrahydroisoquinoline and *N*-(3-Acyloxy-2-benzylpropyl)-*N*′-(4-hydroxy-3-methoxybenzyl) Thioureas Analogues as Potent Vanilloid Receptor Ligands

Ki H. Kim*

Department of Structural Biology, Abbott Laboratories, Abbott Park, IL 60064-6100, USA

Received 10 July 2001; accepted 9 November 2001

Abstract—3-D-Quantitative structure–activity relationships of *N*-(3-acyloxy-2-benzylpropyl)-*N*′-dihydroxytetrahydro-benzazepine and tetrahydroisoquinoline and *N*-(3-acyloxy-2-benzylpropyl)-*N*′-(4-hydroxy-3-methoxybenzyl) thiourea analogues as potent vanilloid receptor ligands were investigated using the CoMFA and the COMSIA methods. The best CoMFA model obtained in this study from 29 substituted thiourea analogues is a two-component model with the following statistics. $R^2_{(cv)} = 0.407$ and $RMSE_{(cv)} = 0.532$ for the cross-validation, and $R^2 = 0.705$ and $RMSE = 0.375$ for the fitted. The best COMSIA model obtained from the same 29 compounds is a two-component model with the following statistics: $R^2_{(cv)} = 0.336$ and $RMSE_{(cv)} = 0.563$ for the cross-validation, and $R^2 = 0.693$ and $RMSE = 0.382$ for the fitted.

Introduction

Capsaicin is the primary pungent component of hot chilli peppers and related plants of the Capsicum family.[1,2] The compound was first isolated in 1876,[3] and the structure was determined in 1919.[4] Capsaicin has a wide spectrum of biological activities including excitatory effects on cardiovascular and respiratory system. It also causes the induction of pain on topical application to skin. These effects are followed by a period of desensitization of sensory neurons producing a long-lasting and naloxone-resistant analgesia. Thus, desensitization of the receptor caused by specific ligands has been considered as a promising therapeutic approach for the treatment of neuropathic pain.

Capsaicin activates vanilloid receptor (VR1). The existence of a vanilloid receptor was first proposed in 1975 from the structure–activity analyses of several capsaicin analogues.[5,6] Subsequently, their existence has been shown from binding studies using a radiolabeled resiniferatoxin (RTX) that mimics most of capsaicin's physiological responses at markedly lower concentration.

Most known VR agonists and antagonists are structurally related to capsaicin and RTX, although fewer VR antagonists are known than agonists. One of the known antagonists is capsazepine, which acts competitively at the capsaicin binding site.[1,7] A number of researchers studied various capsaicin analogues for their analgesic potency. Klopman and Li[8] reported a quantitative structure–activity relationship (QSAR) study of capsaicin analogues as potential agonists with calcium influx activity (EC_{50}) using their MULTIple Computer Automated Structure Evaluation (MULTICASE) methodology.[9] Eq (1) is the QSAR they reported.

$$\begin{aligned}\text{Log}\,(1/EC_{50}) &= 1.29n_1M_1 + 0.40n_2M_2 + 2.45n_3M_3 \\ &\quad - 1.08n_4M_4 - 1.77n_5M_5 - 0.12 \\ &\quad \times (\log P)^2 + 1.23\ \log P - 3.63 \\ N = 70, \quad R^2 &= 0.52, \quad SD = 0.77\end{aligned} \tag{1}$$

In this equation, EC_{50} is the concentration of a drug necessary to produce 50% of the maximal response, M_i

*Tel.: +1-847-937-5797; fax: +1-847-937-2625; e-mail: ki.h.kim@abbott.com

0968-0896/02/$ - see front matter
PII: S0968-0896(01)00404-7

is the *i*th mudulator, n_i is the occurring frequency of M_i in a molecule, and log P is the calculated partition coefficient between octanol and water. They suggested five substructural features in those capsaicin analogues as being responsible for high agonist potency. They also suggested that optimal log P value for the agonist potency is 5.12. The five substructural features are $–CH_2NHC(=S)NHCH_2–$, $–CH_2C(=O)–$ group attached to a phenyl ring, $–NHC(=O)(CH_2)_7–CH=CH–$, part of C_6H_5OH, and –COOH. However, no one reported three-dimensional quantitative structure–activity relationships (3-D-QSAR) of any VR1 agonists or antagonists. Likewise, neither 2-D- nor 3-D-QSAR have been appeared in the literature for the binding affinity of any series of VR1 agonists or antagonists.

Recently, Lee et al. published the synthesis of a series of *N*-(3-acyloxy-2-benzylpropyl)-*N*′-dihydroxytetrahydrobenzazepine and tetrahydroisoquinoline and *N*-(3-acyloxy-2-benzylpropyl)-*N*′-(4-hydroxy-3-methoxybenzyl) thioureas as capsazepin analogues and reported their VR1 binding affinity values. They envisioned these compounds to be structurally mimicking some part of resiniferatoxin.[10,11] We studied three-dimensional quantitative structure–activity relationships of these thiourea analogues. This manuscript describes the 3-D-QSAR results obtained for the binding affinity of these compounds using the technique of Comparative Molecular Field Analysis (CoMFA) and Comparative Molecular Similarity Indices Analysis (COMSIA).

Results and Discussion

The 29 compounds included in this study are listed in Table 1 along with their binding affinity values, K_i, toward VR1. The K_i values were originally determined by competition of [^{3}H]RTX binding using rat VR1 heterologously expressed in CHO cells or dosal root ganglion cultures. In the correlation, the logarithm of $1/K_i$ values, pK_i, was used. Therefore, the larger the pK_i value is, the more potent binder is the compound.

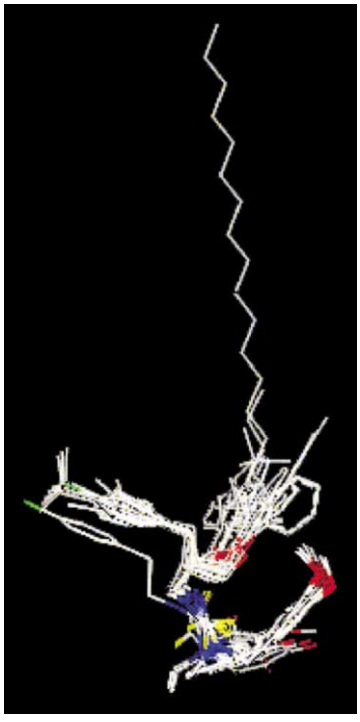

Figure 1. Superimposed position of the substituted thiourea analogues.

The structural feature of compounds **1** and **2** are different from the other compounds in that these compounds do not have CH_2R_1 group as others do. The conformation of the benzyl moiety (left side of the structure as shown in Table 1) of compounds **1**–**13** are rigidified by the cyclization of the group incorporated into a six- or seven-membered ring. The stereochemistry of compounds **3**–**29** on the other end of the molecules is not known. However, the stereoisomers of one compound (**16**) were separated. It was shown that the binding affinity of *R*-isomer is much better than the corresponding *S*-isomer: 18.8 and 74 nM for *R*- and *S*-isomer, respectively. Surprisingly, the K_i value of the mixture is 96 nM, which is weaker than either of the pure isomers. This observation is difficult to understand. Normally, when one isomer is more potent than the other, the binding affinity of the mixture falls in between the two. In any rate, only *R*-isomer of each compound was modeled and used in this 3-D-QSAR analysis. Figure 1 shows all the compounds superimposed over the template group (see Experimental).

The best CoMFA model obtained in this study from 29 substituted thiourea analogues listed in Table 1 is a two-component model with the following statistics: $R^2_{(cv)} = 0.407$ and $RMSE_{(cv)} = 0.532$ for the cross-validation, and $R^2 = 0.705$ and $RMSE = 0.375$ for the fitted. The steric portion of the influences of thiourea analogues for the binding affinity described by this model is 44%, whereas the electrostatic portion is 56%. With a set of scrambled pK_i values (see Experimental) no significant CoMFA model was obtained: (for one-component model) $R^2_{(cv)} = -0.160$, $RMSE_{(cv)} = 0.813$ for the cross-validation, and $R^2 = 0.109$, $RMSE = 0.712$ for the fitted. This supports that the CoMFA model described above was not obtained by chance. Although studied with different compounds, the quality of this CoMFA model can be compared with that of QSAR eq (1) reported for capsaicin analogues by Klopman and Li.[8] The CoMFA model has only two-component whereas eq (1) has seven variables. The CoMFA model also has better squared correlation coefficient and standard error than eq (1). Unlike in eq (1), the lipophilicity of molecule was not found to be important in this CoMFA model.

Upon close examination of the cross-validation results, it was discovered that one compound (**12**) showed an unusually large deviation (−1.149) from the model. This compound is expected to be about 10 times more potent than the observed binding affinity. Exclusion of this compound yielded a CoMFA model with the following statistics: $R^2_{(cv)} = 0.505$, $RMSE_{(cv)} = 0.453$ for the cross-validation, and $R^2 = 0.708$, $RMSE = 0.347$ for the fitted. Although exclusion of compound **12** improved the statistics of the cross-validation, the statistics for the fitted model did not change greatly. The predicted pK_i value

of compound **12** from the CoMFA model obtained from 28 compounds is 6.60 whereas its observed value is 5.15. The types of substituent in compound **12** are not unusual: R_1 = OCO-*t*-Bu, R_2 = 3,4-dimethyl, and R_3 = OH. Other compounds have the same R_1, R_2, or R_3 substituent as compound **12**. For example, compound **10** has the same 3,4-dimethylphenyl substituent at R_2 position, and several other compounds have *t*-Bu group as R_1 position. Eleven of the 29 compounds in Table 1 have OH group as OR_3. Therefore, it is not clear why this compound show an unusually large deviation. On the other hand, it was also observed that Compound **12** is the weakest binder among the compounds included in this study. It is at least 10 times

Table 1. RTX binding affinity (K_i) of capsazepine analogues

No.	Substituent			K_i (μM)	pK_i					Ref: No.
	R_1	R_2	R_3		obs	cal[a]	dev[a]	Cal[b]	Dev[b]	
	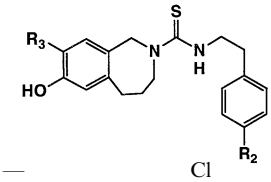									
1	—	Cl	OH	3.22	5.49	5.67	−0.18	5.56	−0.06	8: 12
2	—	Cl	OMe	0.865	6.06	5.73	0.33	5.54	0.52	8: 13
	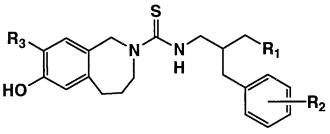									
3	OCOPh	H	OH	0.223	6.66	6.28	0.37	6.28	0.38	8: 14
4	OCOPh	H	OMe	0.590	6.23	6.27	−0.04	6.24	−0.01	8: 15
5	OCO-*t*-Bu	3,4-Me_2	OH	1.156	5.94	6.20	−0.27	6.28	−0.34	8: 16
6	OCO-*t*-Bu	3,4-Me_2	OMe	1.420	5.85	6.18	−0.33	6.25	−0.40	8: 17
	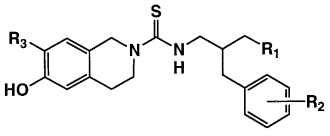									
7	OCOPh	H	OH	0.810	6.09	6.09	0.0026	6.07	0.02	8: 18
8	OCOPh(3,4-Me_2)	H	OH	0.400	6.40	6.37	0.02	6.35	0.04	8: 19
9	OCOPh(4-*t*-Bu)	H	OH	0.520	6.28	6.33	−0.05	6.34	−0.05	8: 20
10	OCOPh	3,4-Me_2	OH	0.627	6.20	6.26	−0.06	6.33	−0.13	8: 21
11	OCOPh	4-*t*-Bu	OH	0.233	6.63	6.54	0.09	6.60	0.04	8: 22
12	OCO-*t*-Bu	3,4-Me_2	OH	7.100	5.15	5.83	−0.68	5.82	−0.67	8: 23
13	OCH2Ph	H	OH	0.267	6.57	6.29	0.28	6.35	0.23	8: 24
	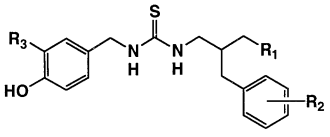									
14	OCOPh	H	OH	0.253	6.60	6.76	−0.16	7.02	−0.42	8: 25
15	OCOPh	H	OMe	0.031	7.51	7.13	0.38	7.11	0.39	8: 26
16	OCO-*t*-Bu	H	OMe	0.096	7.02	7.23	−0.21	7.11	−0.09	9: 18
17	OCO-*i*-Pr	H	OMe	0.133	6.88	7.16	−0.29	7.06	−0.19	9: 19
18	OCO$(CH_2)_4$Me	H	OMe	0.632	6.20	6.14	0.06	6.30	−0.10	9: 20
19	OCO$(CH_2)_{16}$Me	H	OMe	1.870	5.73	5.51	0.21	5.54	0.19	9: 21
20	OCOPh	H	OMe	0.0312	7.51	7.12	0.39	7.10	0.41	9: 22
21	OCO-*t*-Bu	3,4-Me_2	OMe	0.019	7.72	7.12	0.61	7.09	0.63	9: 23, 8: 27
22	OCOPh	3,4-Me_2	OMe	0.410	6.39	7.03	−0.64	7.11	−0.73	9: 24
23	OCOPh(3,4-Me_2)	3,4-Me_2	OMe	0.184	6.74	6.04	0.69	6.22	0.52	9: 25
24	OCO-*t*-Bu	4-Cl	OMe	0.054	7.27	7.28	−0.01	7.18	0.09	9: 26
25	OCOPh	4-Cl	OMe	0.149	6.83	7.16	−0.33	7.16	−0.34	9: 27
26	OCO-*t*-Bu	4-*t*-Bu	OMe	0.0108	7.97	7.43	0.54	7.39	0.58	9: 28, 8: 28
27	OCOPh	4-*t*-Bu	OMe	0.060	7.22	7.24	−0.02	7.29	−0.07	9: 29
28	OCH_2Ph	H	OMe	0.148	6.83	6.83	−0.0046	6.70	0.13	9: 32
29	OCH_2Ph	4-Cl	OMe	0.660	6.18	6.87	−0.69	6.75	−0.56	9: 33

[a]Calculated from the CoMFA model (n = 29, L = 2): $R^2_{(cv)}$ = 0.407 and $RMSE_{(cv)}$ = 0.532 for the cross-validation, and R^2 = 0.705 and RMSE = 0.375 for the fitted.

[b]Calculated from the COMSIA model (n = 29, L = 2): $R^2_{(cv)}$ = 0.336 and $RMSE_{(cv)}$ = 0.563 for the cross-validation, and R^2 = 0.693 and RMSE = 0.382 for the fitted.

weaker than other close analogues listed in Table 1. It is probably worth re-examining the experimental pK_i value of this compound. Since the coefficient contours of the CoMFA model from either 29 or 28 compounds are similar, only the contour plots of the model derived from 29 compounds are shown and discussed below.

Figure 2 is the coefficient contour map of the two-component model derived from all 29 compounds. In this contour map, the sterically favored regions are shown in green, and the sterically disfavored regions are shown in yellow. The positive electrostatic contours are shown in blue, and the negative electrostatic contours are shown in red. Table 1 shows the observed and the calculated pK_i values from this two-component CoMFA model along their observed values. Figure 3a is a plot of the observed and the calculated pK_i values from this model.

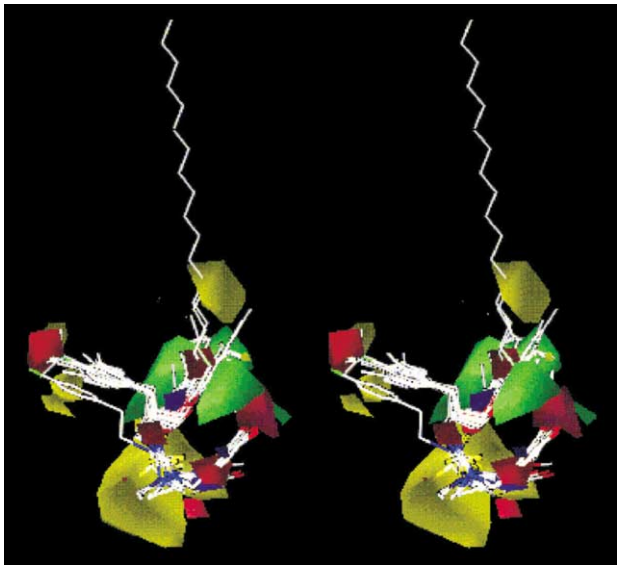

Figure 2. CoMFA coefficient contour map from $n=29$. The sterically favored regions are shown in green, and the sterically disfavored regions are shown in yellow. The positive electrostatic contours are shown in blue, and the negative electrosatic contours are shown in red.

Although the CoMFA model has a moderate statistical quality, its contour plot provides useful information about the structure–activity relationships within this series. The major sterically favored region (colored in green in Fig. 2) is where R_1 group is. In this regard, it is interesting to see that the synthetic chemists quickly learned that the presence of CH_2R_1 is helpful for the increased binding affinity: only compounds **1** and **2** do not have any group at this position. However, a substituent larger than $CH_2OC(=O)$-*t*-Bu group does not appear to be helpful for increasing its binding affinity as can be seen in the two most potent binder, compounds **21** and **26**. The importance of this group could be understood if compound **21** is compared with capsazepine as well as the new ultra-potent antagonist iodo-resiniferatoxin[12] (Fig. 4). Whereas capsazepine lacks $CH_2OC(=O)$-*t*-Bu group, iodo-resiniferatoxin contains a similar moiety, $CH_2C(OH)C(=O)$–$C(=C)CH_3$, which corresponds to $CH_2OC(=O)$-*t*-Bu group (see Fig. 5). It is also known from structure–activity analysis of resiniferatoxin analogues that the αβ-unsaturated α-hydroxyl ketone moiety is important for the potency.[13–15] Especially, reduction of the keto carbonyl group of RTX to hydroxyl group results in a substantial loss of potency.[15] Importance of the carbonyl moiety in $CH_2OC(=O)$-*t*-Bu group is also noted when compound **28** or **29** ($R_1=OCH_2Ph$) is compared with compound **20** or **25** [$R_1=OC(=O)Ph$], respectively. Addition of a long-chain [$CO(CH_2)_{16}Me$] at this position, such as in compound **19**, is not favored and reduced the binding affinity significantly. The sterically disfavored region (colored in yellow in Fig. 2) near the beginning of the long side chain clearly shows this. (See further discussion below on this point.) Figure 2 shows a second sterically favored region near the R_3 position. Only two types of substituent at position R_3 have been investigated in this series: OH and OMe. The green steric contour around the OMe group indicates that OMe is preferred to OH group at least between the two types of substituents. There are four pairs of compounds that can compare the effects of OMe and OH: compounds **1**:**2**, **3**:**4**, **5**:**6**, and **14**:**15**. In two cases (**2** and **15**), OMe is better than OH whereas in the other cases (**3** and **5**), OH is better than OMe. However, on the average, OMe is

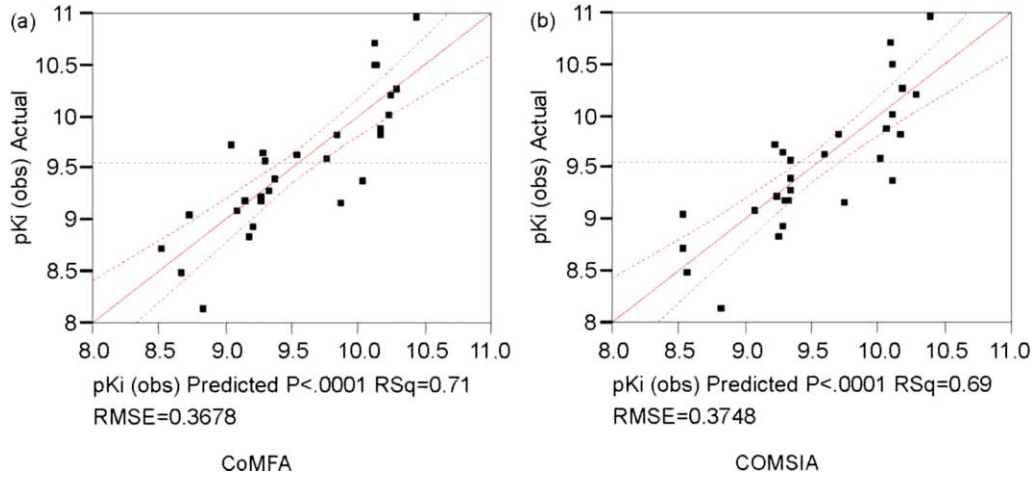

Figure 3. Plots of the observed versus calculated pK_i values using the two-component (a) CoMFA model and (b) COMSIA model.

better than OH, and the CoMFA contours reflect this. Two most potent binders (**21** and **26**) have OMe at this position. The major sterically disfavored region is near the six- or seven-membered ring, which was introduced into the molecule to rigidify the benzyl group of the molecule (left-hand side of the structures in Table 1). The large yellow contours in this region suggest that introduction of two or three methylene units of the six- or seven-membered ring is not beneficial for their binding to the receptor. Since the core molecular area as indicated by the template molecule does not vary, no significant contours are found around this region as expected.

Sometimes an improved 3-D-QSAR model can be obtained with COMSIA, another 3-D-QSAR approach.[16,17] However, with the present set of data very similar results were obtained with this approach. The best COMSIA model obtained from 29 compounds was a two-component model with the following statistics: $R^2_{(cv)} = 0.336$ and $RMSE_{(cv)} = 0.563$ for the cross-validation, and $R^2 = 0.693$ and $RMSE = 0.382$ for the fitted. The steric portion of the influences of thiourea analogues for the binding affinity described by this model is 45%, whereas the electrostatic portion is 55%. With a set of scrambled pK_i values (see Experimental) no significant COMSIA model was obtained. This supports that the COMSIA model described above was also not obtained by chance: (for one-component model) $R^2_{(cv)} = -0.103$, $RMSE_{(cv)} = 0.792$ for the cross-validation, and $R^2 = 0.076$, $RMSE = 0.725$ for the fitted. Although the steric and electrostatic, hydrogen bond donor and acceptor, and hydrophobic fields were initially examined, only the first two fields were found to be important.

Table 1 lists the calculated pK_i values from the two-component COMSIA model. Figure 5 shows the COMSIA coefficient contour map. The sterically favored regions are shown in green, and the sterically disfavored regions are shown in yellow. The positive electrostatic contours are shown in blue, and the negative electrostatic contours are usually shown in red, but almost negligible in this case. The steric contours of the CoMFA contours shown in Figure 3 and the COMSIA contours shown in Figure 5 are very similar. They contain essentially identical information about the steric influences on the binding affinity. It is interesting to see that the COMSIA contour map shows negative steric regions along the long chain [$CO(CH_2)_{16}Me$] of compound **19** at R_1 position. This is consistent with the observation made above that a long R_1 substituent is not favored for increasing binding affinity. More significant differences between the CoMFA and the COMSIA maps are noted for the electrostatic contours. The CoMFA contours show a negative electrostatic region around the hydroxyl or methoxy group at OR_3 position along with the neighboring hydroxyl group. On the other hand, the COMSIA contours show a positive electrostatic region around the NH moiety of thioamide group. It may be possible that the CoMFA and COMSIA contours are complementary rather than discrepancy, and both regions are involved in hydrogen bonding with the receptor: one being hydrogen-bond acceptor and the other being hydrogen-bond donor. This result shows an advantage of investigating 3-D-QSAR with more than one method.

Table 1 lists the calculated pK_i values using the COMSIA model, and Figure 3b is a plot of the observed and the calculated pK_i values from the model.

The CoMFA and COMSIA models obtained in this study are, to our knowledge, the first 3-D-QSAR reported from any vanilloid receptor ligands including

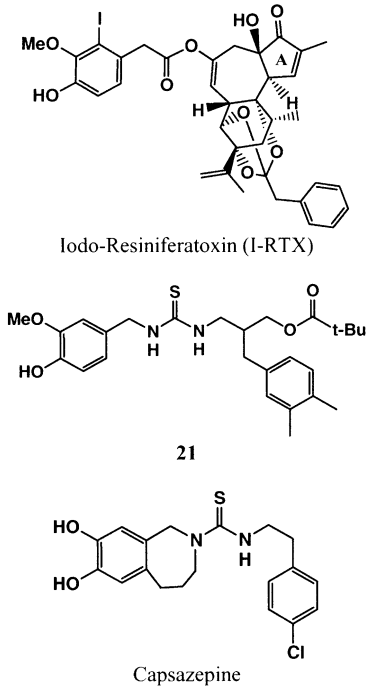

Figure 4. Structure of resiniferatoxin, compound **21**, and capsazepin.

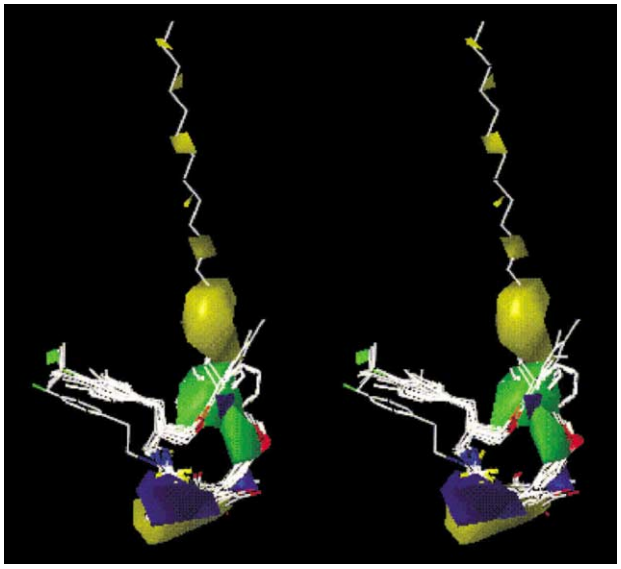

Figure 5. COMSIA coefficient contour map from $n = 29$. The sterically favored regions are shown in green, and the sterically disfavored regions are shown in yellow. The positive electrostatic contours are shown in blue, and the negative electrosatic contours are shown in red (almost negligible).

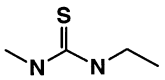

Figure 6. Template structure used for superposition.

the substituted thiourea analogues. It is hoped that the QSAR information reported here would be helpful toward the development of drug working on vanilloid receptor for treatment of pain.

Summary

3-D-Quantitative structure–activity relationships of *N*-(3-acyloxy-2-benzylpropyl)-*N*′-dihydroxytetrahydrobenzazepine and tetrahydroisoquinoline and *N*-(3-acyloxy-2-benzylpropyl)-*N*′-(4-hydroxy-3-methoxybenzyl) thiourea analogues as potent vanilloid receptor ligands were investigated using the CoMFA and the COMSIA methods. Both the CoMFA and the COMSIA approach yielded a two-component model with a similar statistical quality.

Experimental

The molecular modeling of the compounds was done using the molecular modeling package Sybyl (Version 6.7) of Tripos, Inc.[18] The initial geometry of the compounds was built based on capsazepine structure obtained from DISCO program in Sybyl in a study for pharmacophore mapping (manuscript in preparation). These initial geometries were then optimized using the Sybyl minimization procedures with the following options: method = Powell, initial optimization = simplex, termination = gradient, 0.05 kcal/mol, max iterations = 1000, and all others in the default setting of Sybyl 6.6 version.

The atomic point charges were calculated by the Gasteiger–Huckel method implemented in Sybyl. Overlapping the atomic position of the template structure shown in Figure 6 did superposition of the entire molecules. Figure 1 shows all the compounds superimposed over the template moiety. Standard CoMFA Csp^3 probe atom with +1 charge was used with 2 Å grid size for the steric and electrostatic field calculations. The grid box used was created automatically by the program with $X = -3.80$ to 23.08, $Y = -15.49$ to 9.62, and $Z = -5.35$ to 26.37. For the scrambling pK_i values, the compound names and pK_i value columns were first sorted independently. Then, the sorted pK_i values were assigned to the sorted compounds starting from the first compound.

For the COMSIA field calculations, the steric and electrostatic, the donor and acceptor, and the hydrophobic fields were calculated separately with the default attenuation factor (0.3) for the same grid box and size used in CoMFA.

References and Notes

1. Wrigglesworth, R.; Walpole, C. S. J. *Drugs Future* **1998**, *23*, 531.
2. Szolcsanyi, J., Ed. *Handbook of Experimental Pharmacology, Pyretics and Antipyretics*; Springer: Berlin, 1982; p. 437.
3. Thresh, M. *Pharm. J. Trans.* **1876**, 7.
4. Nelson, E. K. *J. Am. Chem. Soc.* **1919**, *41*, 1115.
5. Szolcsanyl, J.; Jancso-Gabor, A. *Arzneimittel-Forsch.* **1975**, *25*, 33.
6. Szolcsanyl, J.; Jancso-Gabor, A. *Arzneimittel-Forsch.* **1975**, *25*, 1877.
7. Szallasi, A.; Blumberg, P. M. *Pharmacol. Rev.* **1999**, *51*, 159.
8. Klopman, G.; Li, J.-Y. *J. Comput.-Aid. Mol. Des.* **1995**, *9*, 283.
9. Klopman, G. *Quant. Struct.-Act. Relat.* **1992**, *11*, 176.
10. Lee, J.; Lee, J.; Szabo, T.; Gonzalez, A. F.; Welter, J. D.; Blumberg, P. M. *Bioorg. Med. Chem.* **2001**, *9*, 1713.
11. Lee, J.; Lee, J.; Kim, J.; Kim, S. Y.; Chun, M. W.; Cho, H.; Hwang, S. W.; Oh, U.; Park, Y. H.; Marquez, V. E.; Beheshti, M.; Szabo, T.; Blumberg, P. M. *Bioorg. Med. Chem.* **2001**, *9*, 19.
12. Wahl, P.; Foged, C.; Tullin, S.; Thomsen, C. *Mol. Pharm.* **2001**, *59*, 9.
13. Szallasi, A.; Sharkey, N. A.; Blumberg, P. M. *Phytother. Res.* **1989**, *3*, 253.
14. Appendino, G.; Cravotto, G.; Palmisano, G.; Annuziata, R.; Szallasi, A. *J. Med. Chem.* **1996**, *39*, 3123.
15. Walpole, C. S. J.; Bevan, S.; Bloomfield, G.; Breckenridge, R.; James, I. F.; Ritchie, T.; Szallasi, A.; Winter, J.; Wrigglesworth, R. *J. Med. Chem.* **1996**, *39*, 2939.
16. Klebe, G.; Abraham, U.; Mietzner, T. *J. Med. Chem.* **1994**, *37*, 4130.
17. Klebe, G. *Perspect. Drug Discov. Des.* **1998**, *12*, 87.
18. Sybyl In Tripos Associates: St. Louis, MO, USA.